Global Journal of Researches in Engineering: C
Chemical Engineering
Volume 15 Issue 3 Version 1.0 Year 2015
Type: Double Blind Peer Reviewed International Research Journal
Publisher: Global Journals Inc. (USA)
Online ISSN: 2249-4596 & Print ISSN: 0975-5861

Chemical and Electrochemical Study on the Effectively of *Melilotus Officinalis* Extract as Save Corrosion Inhibitor for Aluminium in 1 M Hydrochloric Acid Solutions

By Abd El-Aziz S. Fouda, Rabab Abo-Shohba, Walaa M. Husien & Esraa S. Ahmed
Mansoura University, Egypt

Abstract- Melilotus officinalis Extract (MOE), was investigated as a green corrosion inhibitor for aluminium in 1 M HCl solution using weight loss, hydrogen evolution, potentiodynamic polarization, electrochemical impedance spectroscopy (EIS) and electrochemical frequency modulation (EFM) techniques. Surface morphology was tested using scanning electron microscope (SEM). The effect of the temperature on corrosion behavior with addition of different concentrations was studied in the temperature range of 25-45 ^{o}C by weight loss method. Polarization curves reveal that the investigated extract is a mixed type inhibitor. The inhibition efficiency was found to increase with increase in the investigated extract concentration and increase with increase in solution temperature. The adsorption of the inhibitor on aluminium surface was found to obey the Temkin's adsorption isotherm. The activation and adsorption parameters were calculated and discussed. The results obtained from chemical and electrochemical techniques are in good agreement.

Keywords: *acidic corrosion, aluminium, melilotus officinalis extract, EIS, EFM, SEM.*

GJRE-C Classification: *FOR Code: 290699*

Strictly as per the compliance and regulations of:

Chemical and Electrochemical Study on the Effectively of *Melilotus Officinalis* Extract as Save Corrosion Inhibitor for Aluminium in 1 M Hydrochloric Acid Solutions

Abd El-Aziz S. Fouda [α], Rabab Abo-Shohba [σ], Walaa M. Husien [ρ] & Esraa S. Ahmed [ω]

Abstract- Melilotus officinalis Extract (MOE), was investigated as a green corrosion inhibitor for aluminium in 1 M HCl solution using weight loss, hydrogen evolution, potentio-dynamic polarization, electrochemical impedance spectro-scopy (EIS) and electrochemical frequency modulation (EFM) techniques. Surface morphology was tested using scanning electron microscope (SEM). The effect of the temperature on corrosion behavior with addition of different concentrations was studied in the temperature range of 25-45 ºC by weight loss method. Polarization curves reveal that the investigated extract is a mixed type inhibitor. The inhibition efficiency was found to increase with increase in the investigated extract concentration and increase with increase in solution temperature. The adsorption of the inhibitor on aluminium surface was found to obey the Temkin's adsorption isotherm. The activation and adsorption parameters were calculated and discussed. The results obtained from chemical and electrochemical techniques are in good agreement.

Keywords: acidic corrosion, aluminium, melilotus officinalis extract, EIS, EFM, SEM.

I. Introduction

Corrosion is a fundamental process playing an important role in economics and safety, particularly for metals. The use of inhibitors is one of the most practical methods for protection against corrosion, especially in acidic media [1]. Most well-known acid inhibitor are organic compounds containing nitrogen , sulfur, and oxygen atoms. Among them, organic inhibitors have many advantages such as high inhibition efficiency and easy production [2-5]. Organic heterocyclic compounds have been used for the corrosion inhibition of iron [6-9], copper [10], aluminum [11-13], and other metals [14-15] in different corroding media. Although many of these compounds have high inhibition efficiencies, several have undesirable side effects, even in very small concentrations, due to their toxicity to humans, deleterious environmental effects, and high-cost [16].

Author α ω: Department of Chemistry, Faculty of Science, El-Mansoura University, El-Mansoura-35516, Egypt. e-mail: asfouda@hotmail.com
Author σ ρ: Department of Chemistry, Faculty of Science, Al-Azhar University.

Plant extract is low-cost and environmental safe, so the main advantages of using plant extracts as corrosion inhibitor are economic and safe environment. Up till now, many plant extracts have been used as effective corrosion inhibitors for aluminium in acidic media, such as: Garlic [17], Black Mulberry [18], Piper Guineense seed [19] Red onion skin [20]. The inhibition performance of plant extract is normally ascribed to the presence of complex organic species, including tannins, alkaloids and nitrogen bases, carbohydrates and proteins as well as hydrolysis products in their composition. These organic compounds usually contain polar functions with nitrogen, sulfur, or oxygen atoms and have triple or conjugated double bonds with aromatic rings in their molecular structures, which are the major adsorption centers.

Melilotus officinalis extract (MOE), belongs to the family Leguminosae (Fabaceae). It exhibits several medicinal properties, this plant is mainly used for agricultural purposes. It is grown as hay despite its toxic properties when moldy. It is considered an excellent green manure. Sweet clover is a major source of nectar for domestic honey bees. Flowers and seeds can be used as flavoring Melilotus officinalis has been used as a phytoremediation—phytodegradation plant for treatment of soils contaminated with dioxins [21].

The present work was designed to study the inhibitory action of Melilotus officinalis for the corrosion of aluminium in 1 M HCl using Chemical and electrochemical techniques, and to study the effect of temperature on the rate of corrosion

II. Experimental Methods

a) Materials and Solutions

Aluminium used has the chemical composition (% weight) 0.30 Si; 0.60 Fe; 0.10 Cu; 1.40 Mn; 0.05 Mg; 0.05 Cr; 0.05 Ti and the rest aluminium. The auxiliary electrode was a platinum wire (1 cm^2), while a saturated calomel electrode (SCE) connected to a conventional electrolytic cell of capacity 100 ml via a bridge with a Luggin capillary, the tip of which was very close to the surface of the working electrode to minimize the IR drop. The aggressive solution used was prepared by dilution

of analytical reagent grade 37% HCl with bidistilled water. The stock solution (1000 ppm) of Melilotus officinalis was used to prepare the desired concentrations by dilution with bidistilled water. The concentration range of MOE used was 50-300 ppm.

b) Preparation of plant extracts

Fresh aerial parts of MOE sample were crushed to make fine powder. The powdered materials (250 g) were soaked in 500 ml of dichloromethane for 5 days and then subjected to repeated extraction with 5× 50 ml until exhaustion of plant materials. The extracts obtained were then concentrated under reduced pressure using rotary evaporator at temperature below 50°C. The dichloromethane evaporated to give solid extract that was prepared for application as corrosion inhibitor. Chemical studies have demonstrated that the main chemical constituents of Melilotus officinalis are the glycosides of coumaric acid, especially melitoside, which by hydrolysis of lactonises gives coumarin. Free coumarin, 3,4-dihydroxycoumarin (melilotin), scopoletin and umbelliferone are also present [22].

c) Weight loss measurements

Seven parallel aluminium sheets of 2×2×0.2 cm were abraded with emery paper (grade 320–500–1200) and then washed with bidistilled water and acetone. After accurate weighing, the specimens were immersed in a 250 ml beaker, which contained 100 ml of HCl with and without addition of different concentrations of Melilotus officinalis. All the aggressive acid solutions were open to air. After 180 minutes, the specimens were taken out, washed, dried, and weighed accurately. The average weight loss of seven parallel aluminium sheets could be obtained. The inhibition efficiency (IE%) and the degree of surface coverage, θ of MOE for the corrosion of Al were calculated as follows [23]:

$$IE\% = \theta \times 100 = \left[1 - \frac{W}{W^{\circ}}\right] \times 100 \qquad (1)$$

where W° and W are the values of the average weight losses without and with addition of the inhibitor, respectively.

d) Gasometric measurements

The gasometric method assembly used for the measurement of hydrogen gas evolution from the corrosion reaction was designed following the method described by Onuchukwu [24]. The gasometric assembly measures the volume of hydrogen gas evolution from the reaction system. Sevenaluminium coupons of dimension 2 x 2 x 0.2cm were used in the experiments for test solutions containing 1 M HCl with the six different concentrations of MOE and the blank at 25°C. A 50ml of each test solution was introduced into the reaction vessel connected to a burette through a delivery tube. The initial volume of air in the burette was recorded. Thereafter, one aluminium coupon was dropped into the corrodent and the reaction vessel quickly closed. Variation in the volume of hydrogen gas evolved with time was recorded every 1min. for 80 min. Each experiment was conducted on a fresh specimen of metal coupon. The hydrogen gas evolved displaced the paraffin water in the gasometric set-up and the displacement representing the volume of hydrogen evolved was read directly. The experiment was repeated in the presence of the six different concentrations of MOE, 50 to 300 ppm asused in the weight loss experiments.

e) Electrochemical measurements

Electrochemical measurements were performed using a typical three-compartments glass cell consisting of the aluminium specimen as working electrode (1 cm^2), saturated calomel electrode (SCE) as a reference electrode, and a platinum wire as a counter electrode. The reference electrode was connected to a Luggin capillary and the tip of the Luggin capillary is made very close to the surface of the working electrode to minimize IR drop. All the measurements were done in solutions open to atmosphere under unstirred conditions. All potential values were reported versus SCE. Prior to each experiment, the electrode was abraded with successive different grades of emery paper, degreased with acetone, also washed with bidistilled water, and finally dried. Tafel polarization curves were obtained by changing the electrode potential automatically from (-0.8 to 1 V vs. SCE) at open circuit potential with a scan rate of 1 mVs^{-1}. Stern-Geary method [25], used for the determination of corrosion current is performed by extrapolation of anodic and cathodic Tafel lines to a point which gives (log i_{corr}) and the corresponding corrosion potential (E_{corr}) for inhibitor free acid and for each concentration of inhibitor. Then (i_{corr}) was used for calculation of inhibition efficiency (IE %) and surface coverage (θ) as in equation 2:

$$IE\% = \Theta \times 100 = \left[1 - \frac{i_{corr\ (inh)}}{icorr_{\ (free\ )}}\right] \times 100 \qquad (2)$$

Where $i_{corr(free)}$ and $i_{corr(inh)}$ are the corrosion current densities in the absence and presence of inhibitor, respectively.

Impedance measurements were carried out in frequency range ($2x10^4$ Hz to $8x10^{-2}$ Hz) with amplitude of 5 mV peak-to-peak using AC signals at open circuit potential. The experimental impedance was analyzed and interpreted based on the equivalent circuit. The main parameters deduced from the analysis of Nyquist diagram are the charge transfer resistance R_{ct} (diameter of high-frequency loop) and the double layer capacity C_{dl}. The inhibition efficiencies and the surface coverage (θ) obtained from the impedance measurements are calculated from equation 3:

$$IE\% = \Theta \times 100 = \left[1 - \left(\frac{R^{\circ}_{ct}}{R_{ct}}\right)\right] \times 100 \qquad (3)$$

Where R^{o}_{ct} and R_{ct} are the charge transfer resistance in the absence and presence of inhibitor, respectively.

Electrochemical frequency modulation, EFM, was carried out using two frequencies 2 and 5 Hz. The large peaks were used to calculate the corrosion current density (i_{corr}), the Tafel slopes (β_a and β_c) and the causality factors CF-2&CF-3 [26]. The electrode potential was allowed to stabilize 30 min before starting the measurements. All the experiments were conducted at 25°C.

All electrochemical measurements were performed using Gamry Instrument (PCI4/750) Potentiostat/ Galvanostat/ZRA. This includes a Gamry framework system based on the ESA 400. Gamry applications include DC105 software for potentio-dynamic polarization, EIS 300 software for electro-chemical impedance spectroscopy, and EFM 140 software for electrochemical frequency modulation measurements via computer for collecting data. Echem Analyst 6.03 software was used for plotting, graphing, and fitting data. To test the reliability and reproducibility of the measurements, duplicate experiments, which performed in each case at the same conditions.

f) Surface morphology

For morphological study, surface features (2 x 2 x 0.2cm) of aluminium were examined before and after exposure to 1 M HCl solutions for 24 hour with and without extract. JEOL JSM-5500 scanning electron microscope was used for this investigation.

III. Results and Discussion

a) Weight loss measurements

Weight loss measurements were carried out for aluminium in 1 M HCl in the absence and presence of different concentrations of Melilotus officinalis and are shown in Figure (1). The inhibition efficiency (IE%) values calculated are listed in Table (1). From this table, it is noted that the IE% increases steadily with increasing the concentration of *Melilotus officinalis* and with increasing temperature from 25-45°C. The inhibition efficiency (IE%) and surface coverage (θ)were calculated by equation (1). The observed inhibition action of the MOE could be attributed to the adsorption of its components on aluminium surface. The formed layer, of the adsorbed molecules, isolates the metal surface from the aggressive medium which limits the dissolution of the latter by blocking of their corrosion sites and hence decreasing the corrosion rate, with increasing efficiency as their concentrations increase [27].

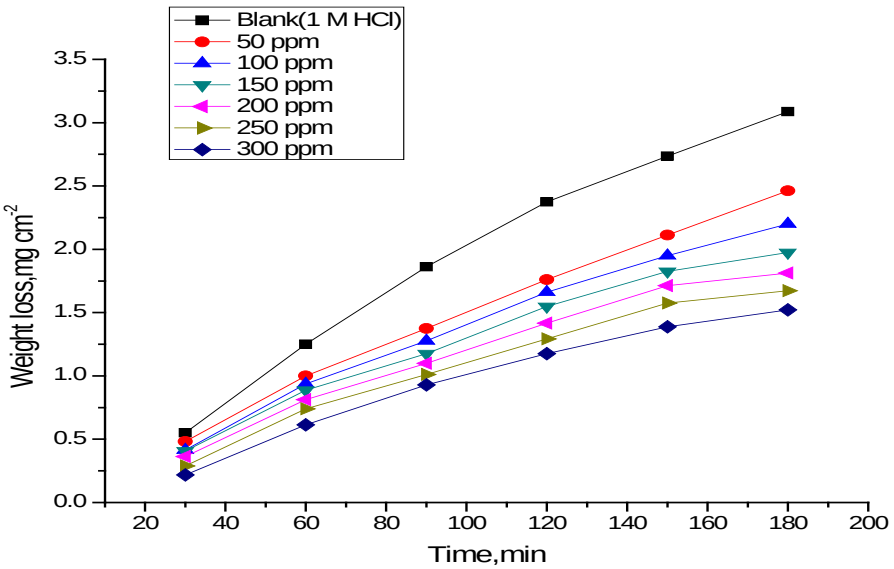

Figure 1 : Weight loss-time curves for the corrosion of aluminium in 1 M HCl in the absence and presence of different concentrations of MOE at 25°C

b) Gasometric measurements

The volume of hydrogen evolved during the corrosion reaction of aluminium in 1 M HCl solutions devoid of and containing different concentrations of extract is measured as a function of the reaction time, and the data are represented graphically in Figure 2. Inspection of the figure reveals that, the hydrogen evolution starts after a certain time from the immersion of aluminum coupon in the test solution. It may be expected thatthis time corresponds to the period needed by the acid to destruct the pre-immersion oxide film before the start of the metal attack, and it is known

as the incubation period. Further inspection of Figure 2 reveals linear relationship between the time of reaction and the volume of hydrogen evolved, in all of the tested solutions. However, the presence of the extract decreases, markedly, the slope of the straight line. Since the slope of the line represents the corrosion reaction rate, it could be concluded that the *Melilotus offecinalis* extract has an excellent ability to inhibit the corrosion of aluminium in the acid solution. The values of inhibition efficiencies of different concentrations of the extract are given in Table 2. Inspection of Table 2 reveals that the IE increases as the concentration of the extract is increased.

Table 1 : Variation of corrosion rate (k_{corr}), surface coverage(Θ)and inhibition efficiency(IE%) with different concentrations of MOE after 120 minutes of immersion in 1 M HCl at different temperatures.

Temp. °C	[Inh] ppm	Weight loss, mg cm^{-2}	k_{corr}, mg cm^{-2} min^{-1}	Θ	
25	Blank	3.24	0.027	-----	-----
	50	1.48	0.012	0.544	54.4
	100	1.46	0.012	0.546	54.6
	150	1.41	0.011	0.560	56.0
	200	1.31	0.011	0.599	59.9
	250	1.30	0.011	0.595	59.5
	300	1.20	0.010	0.623	62.3
30	Blank	7.44	0.062	----	-----
	50	2.55	0.021	0.657	65.7
	100	2.41	0.020	0.674	67.4
	150	2.22	0.020	0.701	70.1
	200	1.81	0.018	0.757	75.7
	250	1.73	0.014	0.767	76.7
	300	1.66	0.013	0.776	77.6
35	Blank	23.67	0.198	----	-----
	50	6.70	0.055	0.717	71.7
	100	6.49	0.054	0.726	72.6
	150	6.10	0.050	0.744	74.4
	200	5.24	0.043	0.778	77.8
	250	4.87	0.040	0.794	79.4
	300	4.39	0.036	0.814	81.4
40	Blank	34.92	0.291	-----	-----
	50	5.82	0.049	0.834	83.4
	100	5.39	0.044	0.845	84.5
	150	4.55	0.037	0.869	86.9
	200	4.10	0.034	0.883	88.3
	250	3.65	0.030	0.895	89.5
	300	3.25	0.027	0.907	90.7
45	Blank	51.96	0.433	-----	-----
	50	8.10	0.068	0.845	84.5
	100	7.35	0.061	0.858	85.8
	150	6.50	0.054	0.874	87.4
	200	5.57	0.046	0.893	89.3
	250	4.75	0.039	0.908	90.8
	300	3.80	0.032	0.926	92.6

Table 2 : Inhibition efficiency obtained from hydrogen evolution method for Al after 80 minutes from immersion in 1 M HCl for various concentrations of MOEat 25°C

[Inh] Ppm	Volume of hydrogen gas evolvedml	IE %
Blank	6.3	-
50	2.7	56.8
100	2.4	61.9
150	2.1	66.6
200	1.8	72.2
250	1.4	77.7
300	1.1	83.3

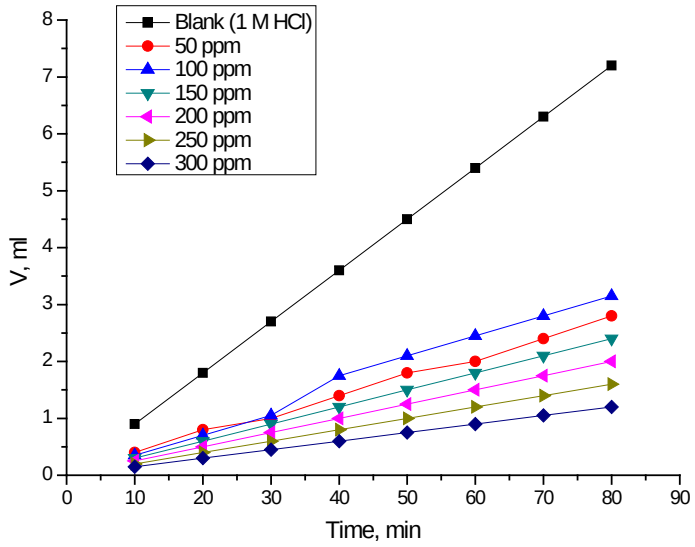

Figure 2 : volume of hydrogen gas evolved during the corrosion of aluminium in 1M HCl in the absence and presence of different concentrations of MOE

c) *Polarization curves*

Figure 3 shows potentiodynamic polarization curves recorded for aluminium in 1 M HCl solutions in the absence and presence of various concentrations of MOE at 25°C.

Lee and Nobe [28] reported the occurrence of a current peak between the apparent-Tafel and limiting-current regions during potential sweep experiments. The presence of MOE shifts both anodic and cathodic branches to the lower values of corrosion current densities and thus causes a remarkable decrease in the corrosion rate. The parameters derived from the polarization curves in Figure 3 are given in Table 3. In 1 M HCl solution, the presence of MOE causes a remarkable decrease in the corrosion rate i.e., shifts both anodic and cathodic curves to lower current densities. In other words, both cathodic and anodic reactions of aluminium electrode are retarded by MOE in 1 M HCl solution. The Tafel slopes of β_a and β_c at 25°Cdo not change remarkably upon addition of MOE, which indicates that the presence of MOE does not change the mechanism of hydrogen evolution and the metal dissolution process. Generally, an inhibitor can be classified as cathodic type if the shift of corrosion potential in the presence of the inhibitor is more than 85 mV with respect to that in the absence of the inhibitor [29, 30]. In the presence of MOE, E_{corr} shifts to less negative but this shift is very small (about 20-30 mV), which indicates that MOE can be arranged as mixed inhibitor.

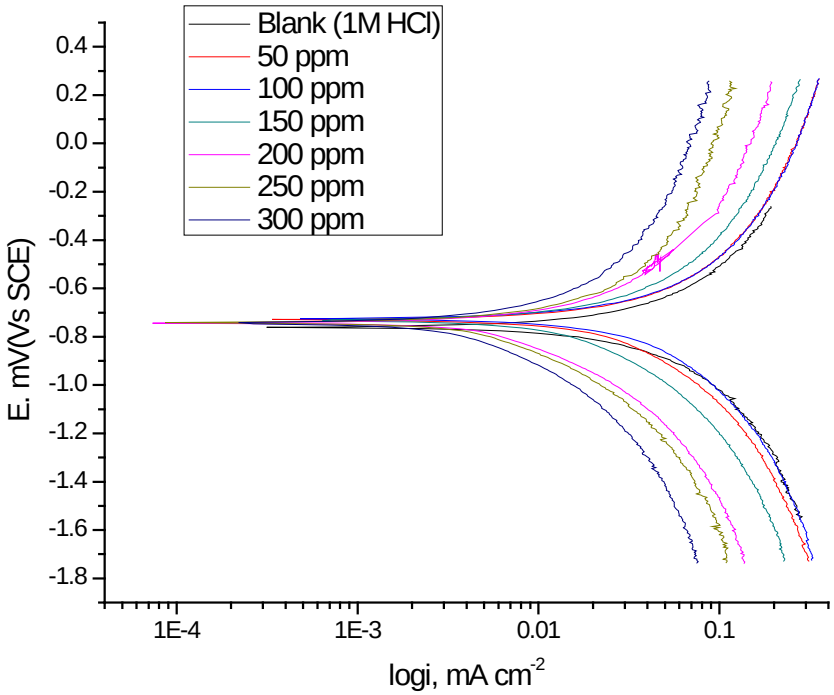

Figure 3 : Potentiodynamic polarization curves for the corrosion of aluminium in 1 M HCl solution without and with various concentrations of MOE at 25˚C

Table 3 : Corrosion potential (E_{corr}), corrosion current density (i_{corr}), Tafel slopes (β_c,β_a), degree of surface coverage (θ), and inhibition efficiency (IE%) of Al in 1M HCl at 25°C

[Inh] ppm	$-E_{corr}$ mV vs SCE	i_{corr} m A cm^{-2}	β_a mV dec^{-1}	β_c mV dec^{-1}	C.Rx10^{-3} mpy	θ	IE%
0	725	275	250	420	164	---	---
50	760	136	150	170	58	0.505	50.5
100	730	127	80	100	57	0.538	53.8
150	732	82	60	100	37	0.700	70.0
200	743	62	30	90	10	0.773	77.3
250	742	56	20	90	5.3	0.796	79.6
300	744	30	30	90	5.0	0.889	88.9

d) Electrochemical impedance spectroscopy (EIS) measurements

Figure 4 shows impedance plots for aluminium in 1 M HClsolution without and with different concentrations of MOE. The impedance spectra consists of a Nyquist semicircle type without appearance of diffusive contribution to the total impedance (Z) indicating that the corrosion proceeds mainly under charge-transfer control and the presence of extract do not alter the mechanism of corrosion reaction.It is found that the obtained Nyquist plots are not perfect semicircle due to frequency dispersion and this behavior can be attributed to roughness and in homogeneities of the electrode surface [31, 32]. When there is non-ideal frequency response, it is common practice to use distributed circuit elements in an equivalent circuit. The most widely employed is the constant phase element (CPE). In general a CPE is used in a model in place of a capacitor to compensate for inhomogeneity in the system [33]. It was found that the diameters of the semicircle increases with increasing the concentration of the investigated extract. This indicates that the polarization resistance of the oxide layer increases with increasing the concentration of MOE and the depressed capacitive semicircle are often referred to the surface roughness and inhomogeneity, since this capacitive semicircle is correlated with dielectric properties and thickness of the barrier oxide film [34]. The data revealed that, each impedance diagram consists of a large capacitive loop with low frequencies dispersion (inductive arc). This inductive arc is generally attributed to anodic adsorbed intermediates controlling the anodic process [35-36]. By following this, inductive arc was disregarded. The electrical equivalent circuit model shown in Figure 5 was used to analyze the obtained impedance data. The model consists of the

solution resistance (R_s), the charge-transfer resistance of the interfacial corrosion reaction (R_{ct}) and the constant phase angle element (CPE). The value of frequency power (n) of CPE can be assumed to correspond to capacitive behavior. However, excellent fit with this model was obtained with our experimental data. The admittance of CPE is described as:

$$Y_{CPE} = Y_o(j\omega)^n \quad (4)$$

where j is the imaginary root, ω the angular frequency, Y_o the magnitude and *n* the exponential term [37].

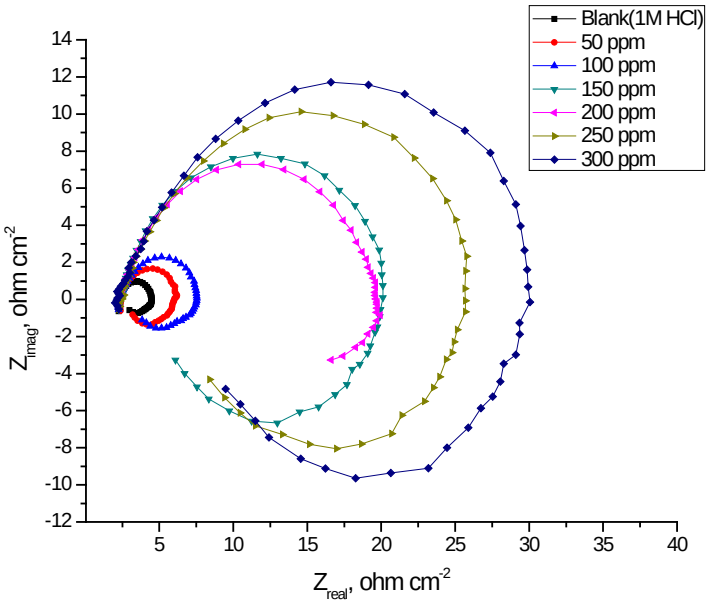

Figure 4 : Nyquist plots for aluminium in 1 M HCl solutions in the absence and presence of various concentrations of MOE at 25°C

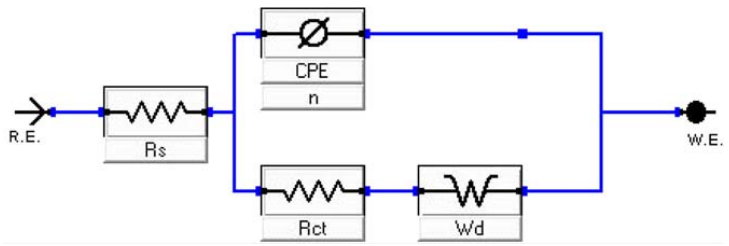

Figure 5 : Equivalent circuit used to model impedance data for aluminium in 1 M HCl solutions

A long Warburg diffusion tail was observed at low frequency values. The tails are inclined at an angle of 45° to the real-axis at the very low frequencies; A diffusion controlled process is therefore exists. Studies reported in the literature [38] showed that the diffusion process is controlled by diffusion of dissolved oxygen from the bulk solution to the electrode surface and the Warburg impedance, which is observed in the low frequency regions, is ascribed to diffusion of oxygen to the alloy surface. This diffusion tail still appears, even in presence of high concentrations of the investigated extract. This means that the corrosion behavior of alloy in the absence as well as in the presence of MOE is influenced by mass transport.

Also, Bode plots for the aluminium in 1 M HCl solution are shown in Figure 6. In which the high frequency limit corresponding to the electrolyte resistance (ohmic resistance) R_Ω, while the low frequency represents the sum of (R_Ω + R_{ct}), where R_{ct} is in the first approximation determined by both electrolytic conductance of the oxide film and the polarization resistance of the dissolution and repassivation process. At both low and high frequency limits, the phase angle between the current and potential (θ), assumes a value of about 0°, corresponding to the resistive behavior of R_Ω and (R_Ω + R_{ct}).

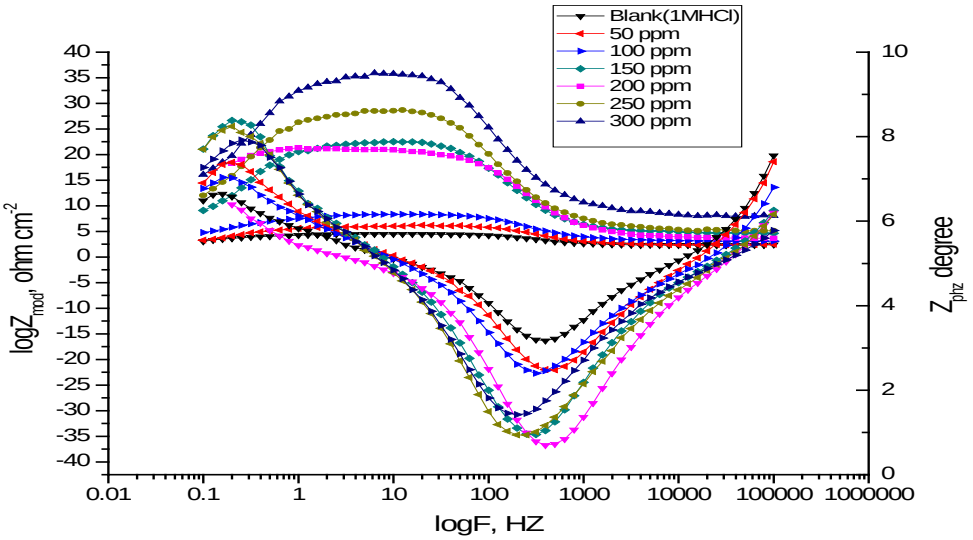

Figure 6 : Bode plots for aluminium in 1 M HCl solutions in the absence and presence of various MOE concentrations at 25°C

The main parameters deduced from the analysis of Nyquist diagram are:

- The resistance of charge transfer R_{ct}(diameter of high frequency loop)
- The capacity of double layer C_{dl} which is defined as :

$$C_{dl} = \frac{1}{2\pi R_{ct} f_{max}} \quad (5)$$

Where f_{max} is the maximum frequency at which the Z_{imag} of the impedance is a maximum. Since the electrochemical theory assumed that ($1/R_{ct}$) is directly proportional to the capacity of double layer C_{dl}, the inhibition efficiency (IE%) of the inhibitor for aluminium in 1 M HCl solution was calculated from R_{ct} values obtained from impedance data at different inhibitor concentration the following equation:

$$IE\% = \left(1 - \frac{R^{\circ}_{ct}}{R_{ct}}\right) \times 100 \quad (6)$$

Where R°_{ct} and R_{ct} are the charge transfer resistance in the absence and Presence of investigated extract, respectively. From the impedance data given in Table 4, we can conclude that the value of R_{ct} increases with the increase in the concentration of the investigated extract and this indicates the formation of a protective film on the Al surface by the adsorption and an increase in the corrosion inhibition efficiency in acidic solution. While the value of C_{dl} decreases with increasing the concentrations of extract in comparison with that of blank solution (uninhibited), as a result from the replacement of water molecules by inhibitor molecules which lead to increase in local dielectric constant and/or an increase in the thickness of the electric double layer formed on the metal surface [39,40].

Table 4 : Electrochemical kinetic parameters obtained from EIS technique for Al in 1M HCl in the absence and presence of different concentrations of investigated plant extracts at 25°C

[Inh] ppm	R_p Ω Cm^2	$C_{dl}x10^{-6}$ $\mu F\ Cm^{-2}$	Θ	IE%
0	1.7	21	---	---
50	2.9	5.9	0.468	46.8
100	3.2	4.4	0.595	59.5
150	4.2	3.2	0.730	73.0
200	6.3	3.0	0.760	76.0
250	7.1	2.5	0.840	84.0
300	10.9	2.3	0.844	84.4

e) Electrochemical frequency modulation (EFM) measurements

EFM is a nondestructive corrosion measurement technique that can directly determine the corrosion current value without prior knowledge of Tafel slopes, and with only a small polarizing signal. These advantages of EFM technique make it an ideal candidate for online corrosion monitoring [41]. The great strength of the EFM is the causality factors which serve as an internal check on the validity of EFM measurement. The causality factors CF-2 and CF-3 are calculated from the frequency spectrum of the current

responses. Figure 7 show the frequency spectrum of the current response of pure Aluminium in 1 M HCl solution, contains not only the input frequencies, but also contains frequency components which are the sum, difference, and multiples of the two input frequencies. The EFM intermodulation spectrums of Aluminium in 1 M HCl solution containing (50ppm- 300ppm) of the MOE extract at 25°C is shown in Figure 7. The harmonic and intermodulation peaks are clearly visible and are much larger than the background noise. The two large peaks, with amplitude of about 200 μA, are the response to the 40 and 100 mHz (2 and 5 Hz) excitation frequencies. It is important to note that between the peaks there is nearly no current response (<100 mA). The experimental EFM data were treated using two different models: complete diffusion control of the cathodic reaction and the "activation" model. For the latter, a set of three non-linear equations had been solved, assuming that the corrosion potential does not change due to the polarization of the working electrode [42]. The larger peaks were used to calculate the corrosion current density (i_{corr}), the Tafel slopes (β_c and β_a) and the causality factors (CF-2 and CF-3).These electrochemical parameters were simultaneously determined by Gamry EFM 140 software, and listed in Table 5 indicating that this extract inhibit the corrosion of aluminium in 1 M HCl through adsorption. The causality factors obtained under different experimental conditions are approxi-mately equal to the theoretical values (2 and 3) indicating that the measured data are verified and of good quality [43]. The inhibition efficiencies IE_{EFM} % increase by increasing the studied extract concentrations and was calculated as follows:

$$IE\ \%_{EFM} = \left(1 - \frac{i_{corr}}{i^{o}_{corr}}\right) \times 100 \quad (7)$$

Where i^{o}_{corr} and i_{corr} are corrosion current densities in the absence and presence of MOE extract, respectively.

Table 5 : Electrochemical kinetic parameters obtained from EFM technique for aluminium in 1M HCl in the absence and presence of different concentrations of MOE

[Inh] ppm	i_{corr} m A cm^{-2}	β_a mV dec^{-1}	β_c mV dec^{-1}	CF-2	CF-3	CRx10^{-3} mpy	θ	IE%
0	1100	182	195	1.1	2.3	667	---	---
50	400.9	32	102	2.0	2.7	238	0.642	64.2
100	348.8	31	66	1.1	2.9	207	0.688	68.8
150	345.7	34	55	1.7	2.2	204	0.691	69.1
200	342.8	24	36	1.8	2.5	146	0.694	69.4
250	235.5	19	33	1.2	2.3	140	0.789	78.9
300	214.3	18	25	2.0	2.3	127	0.809	80.9

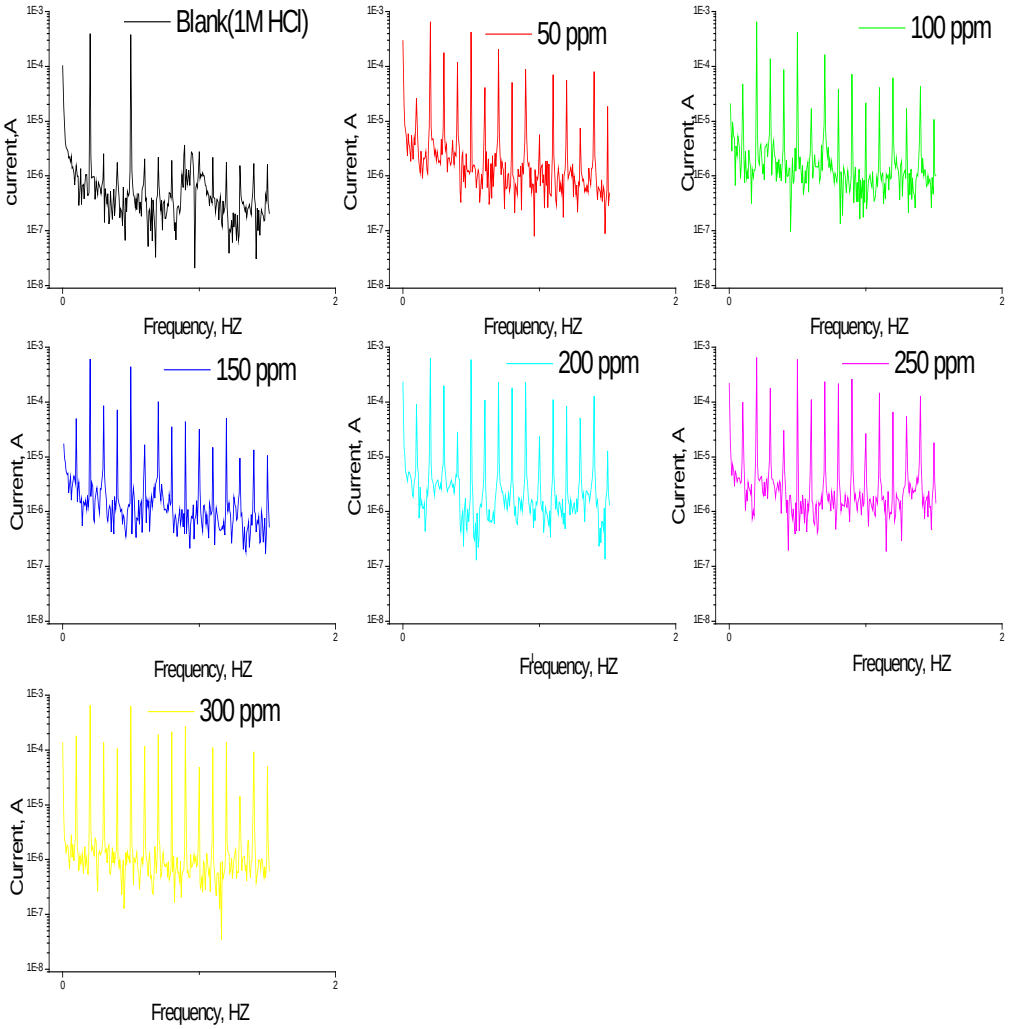

Figure 6 : Intermodulation spectrums for the corrosion of aluminium in 1 M HCl without and with various concentrations of MOE at 25˚C.

f) Adsorption isotherms

The mode and interaction degree between an inhibitor and a metallic surface have been widely studied with the application of adsorption isotherms. The adsorption of an organic molecule occurs because the interaction energy between an inhibitor and a metallic surface is higher than that between water molecules and metallic surface [44, 45]. To obtain the adsorption isotherms, the degree of surface coverage (θ) obtained from weight loss method was determined as a function of inhibitor concentration. The values of θ were then plotted to fit the most suitable model of adsorption [46]. Attempts were made tofit experimental data to various isotherms including Frumkin, Langmuir, Temkin, Freundlich, isotherms. By far the results were bestfitted by Temkin adsorption isotherm as seen in Figure 7 [47].

$$a/2.303\Theta = \log K_{ads} + \log C \qquad (9)$$

The equilibrium constant of adsorption K_{ads} obtained from the intercepts of Temkin adsorption isotherm is related to the free energy of adsorption ΔG° ads as follows:

$$K_{ads} = 1/55.5 \exp[(-\Delta G^{\circ}_{ads})/ RT] \qquad (8)$$

where 55.5 is the molar concentration of water in the solution in M^{-1}.The values obtained are given in Table 6.

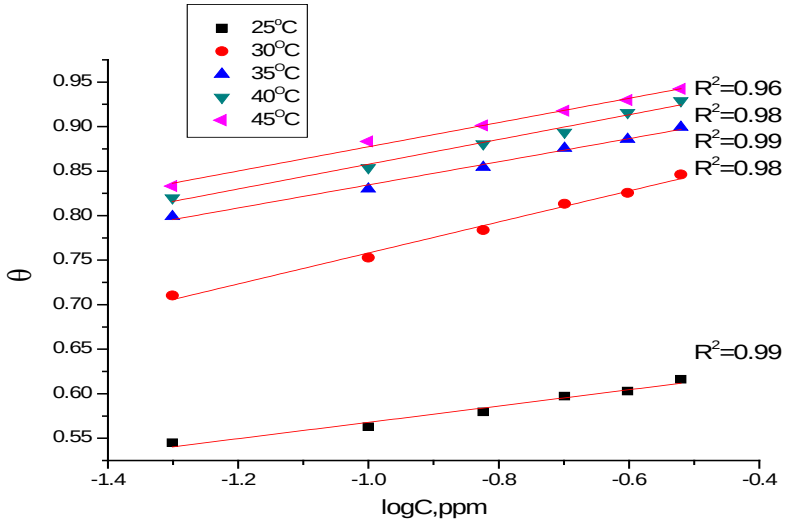

Figure 7 : Temkin adsorption plots for aluminium in 1 M HCl containing various concentrations of MOE at 25°C

Plot of (ΔG^{o}_{ads}) versus T (Figure 8) gave the heat of adsorption (ΔH^{o}_{ads}) and the entropy (ΔS^{o}_{ads}) according to the thermodynamic basic equation 5:

$$\Delta G^{o}_{ads} = \Delta H^{o}_{ads} - T\,\Delta S^{o}_{ads} \quad (5)$$

Table 6 clearly shows a good dependence of ΔG^{o}_{ads} on T, indicating the good correlation among thermodynamic parameters. The negative value of ΔG^{o}_{ads} reflect that the adsorption of studied inhibitors on aluminium surface from 1 M HCl solution is spontaneous process and stability of the adsorbed layer on the aluminium surface. Generally, values of ΔG^{o}_{ads} around -20 kJ mol^{-1} or lower are consistent with the electrostatic interaction between the charged molecules and the charged metal (physical adsorption); those around -40 kJ mol^{-1} or higher involves charge sharing or transfer from organic molecules to the metal surface to form a coordinate type of bond (chemisorption) [48]. From the obtained values of ΔG^{o}_{ads} it was found the existence of chemical adsorption). The values of thermodynamic parameter for the adsorption of inhibitors Table 6 can provide valuable information about the mechanism of corrosion inhibition. Endothermic adsorption process ($\Delta H^{o}_{ads} > 0$) is attributed unequivocally to chemisorption [49], an exothermic adsorption process ($\Delta H^{o}_{ads} < 0$) may involve either physisorption or chemisorption or mixture of both processes. In the presented case, the calculated values of ΔH^{o}_{ads} for the adsorption of extract in 1 M HCl indicating that this extract may be chemically adsorbed. The values of ΔS^{o}_{ads} in the presence of extract is large and positive that is accompanied with endothermic adsorption process. This indicates that decrease in disorder takes places on going from reactants to the metal-adsorbed reaction complex [50].

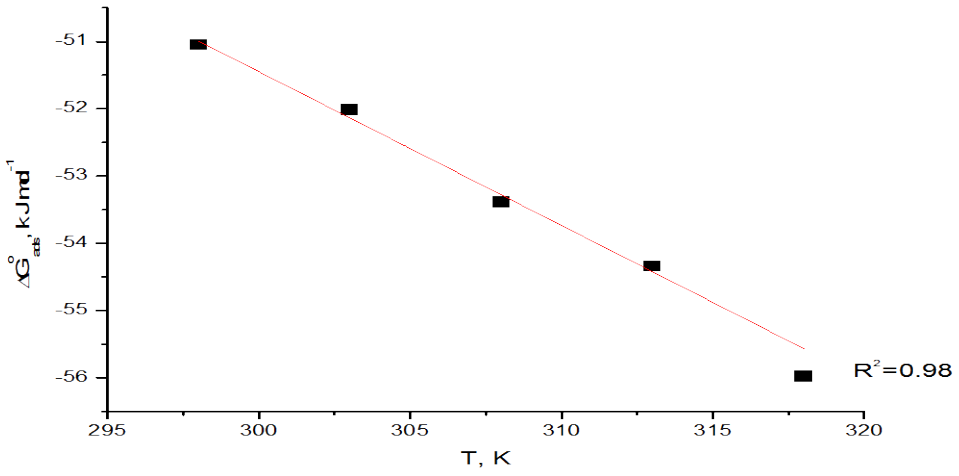

Figure 8 : Variation of ΔG^{o}_{ads} versus T for the adsorption of MOE on aluminium surface in 1 M HCl at different temperatures

Table 6 : Thermodynamic parameters for the adsorption of MOE on aluminium in 1MHCl at different temperatures.

Temp. °C	$K_{ads}x10^{-6}$ M^{-1}	$-\Delta G^{o}_{ads}$ k J mol^{-1}	$-\Delta H^{o}_{ads}$ k J mol^{-1}	ΔS^{o}_{ads} J mol^{-1} k^{-1}
25	12.2	50.4	17.2	226.7
30	15.6	51.8		227.8
35	20.6	53.4		229.2
40	26.9	54.9		230.5
45	33.9	56.5		231.6

g) Kinetic-thermodynamic corrosion parameters

Weight loss method was carried out at different temperature (25°C–45°C) in the presence of different concentration of MOE. It has been found that he corrosion rate decreases with the increase in temperature for MOE (Table 1). The corrosion rate of aluminium in the absence of MOE increased steeply from 25 to 45°Cwhereas; in the presence of MOE the corrosion rate decreased slowly. The inhibition efficiency was found to increase with temperature. The corrosion parameter in the absence and presence of extract in the temperature range 25–45°C has been summarized in (Table 1).The apparent activation energy (E^{*}_{a}) for dissolution of aluminium in 1 M HCl was calculated from the slope of plots by using Arrhenius equation:

$$\log k = \frac{-E_a^*}{2.303\ R\ T} + \log A \qquad (9)$$

where k is rate of corrosion, E^{*}_{a} is the apparent activation energy, R is the universal gas constant, T is absolute temperature and A is the Arrhenius pre-exponential factor.

By plotting log k against 1/T the values of activation energy (E^{*}_{a}) has been calculated (E^{*}_{a} = (slope) 2.303 x R) (Figure 9). Activation energy for the reaction of aluminium in 1M HCl decreases in the presence of extract (Table 7). This decreas indicates the formation of chemical bonds were strengthen by increasing the temperature. However, the extent of the rate increment in the inhibited solution is lower than that in the free acid solution. Therefore, the inhibition efficiency of the MOE increases markedly with increasing temperature. This result supports the idea that the adsorption of extract components on the aluminium surface may be chemical in nature. Thus, as the temperature increases the number of adsorbed molecules increases leading to an increase in the inhibition efficiency. This could be done by adsorption on the aluminium surface making a barrier for mass and charge transfer. However, such types of inhibitors perform a good inhibition at high temperature with considerable increase in inhibition efficiency at elevated temperatures [51]. Moreover, the relatively high value of activation energy in presence of MOE suggests a chemical adsorption process.

The values of change of entropy (ΔS^{*}) and change of enthalpy (ΔH^{*}) can be calculated by using the formula:

$$k = \left(\frac{RT}{Nh}\right) exp\left(\frac{\Delta S^*}{R}\right) exp\left(\frac{\Delta H^*}{RT}\right) \qquad (10)$$

where k is rate of corrosion, h is Planck's constant, N is Avogadro number, ΔS^{*} is the entropy of activation, and ΔH^{*} is the enthalpy of activation. A plot of log (k/T) vs. 1/T (Figure 10) should give a straight line, with a slope of (ΔH^{*}/2.303R) and an intercept of [log (R/Nh)+ΔS^{*}/ 2.303R], from which the values of ΔS^{*} and ΔH^{*} can be calculated (Table 7). The positive value of ΔS^{*} for the extract indicates that activated complex in the rate determining step represents a dissociation rather than an association step, meaning that an increase in disorder takes place during the course of transition from reactant to the activated complex [52] The positive sign of ΔH^{*} indicates that the adsorption of extract molecules is an endothermic process. Generally, an endothermic process signifieschemisorption process.

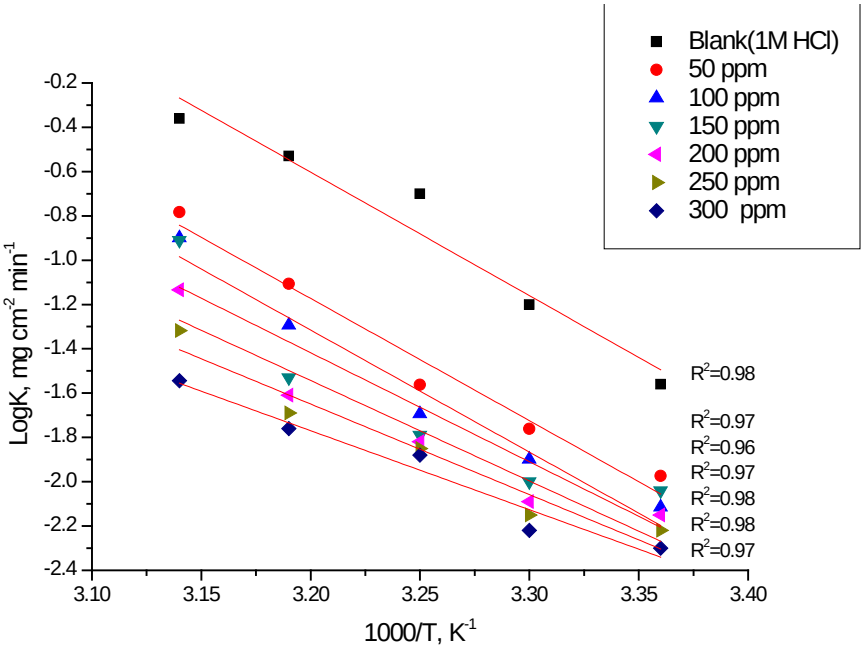

Figure 9 : log k (corrosion rate) – 1/T curves for aluminium in 1 M HCl in the absence and presence of different concentrations of MOE

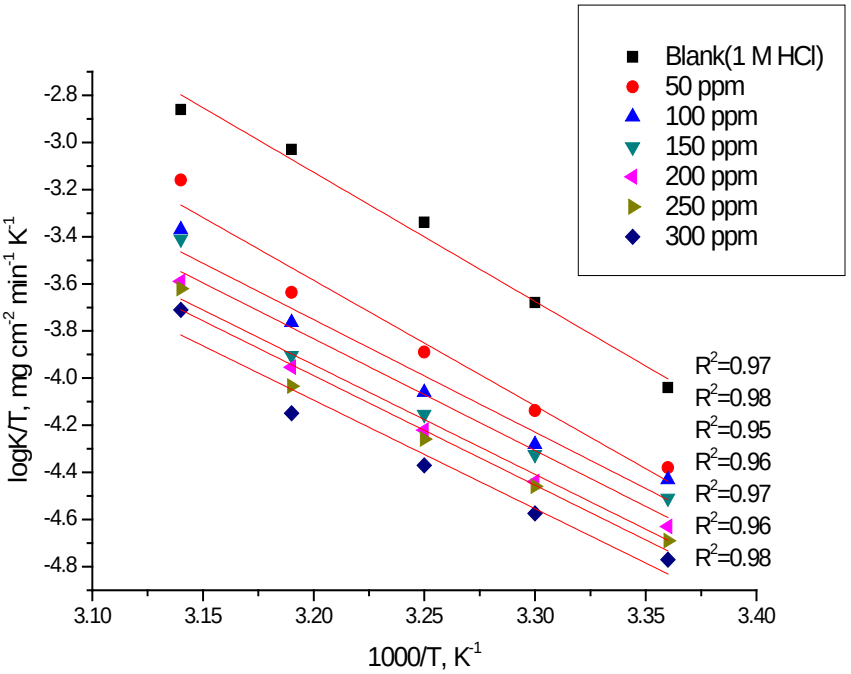

Figure 10 : log k (corrosion rate) /T – 1/T curves for aluminium in 1 M HCl in the absence and presence of different concentrations of MOE

Table 7 : Activation parameters for dissolution of aluminium in the absence and presence of different concentrations of MOE in 1 M HCl

Conc. ppm	E_a^*, kJ mol^{-1}	ΔH^*, kJ mol^{-1}	ΔS^*, J mol^{-1}K^{-1}
1 M HCl	106.6	45.5	78.1
50	105.5	44.3	60.1
100	105.3	39.7	23.2
150	94.2	39.4	19.4
200	86.7	38.6	11.7
250	78.1	38.5	10.7
300	68.1	38.2	6.1

h) Surface analysis by scanning electron microscopy

Figure11shows an SEM photograph recorded for aluminium samp-les polished (a) and exposed for 24 h in 1 M HCl solution without (b) and with (c) 300 ppm of MOE at 25C^0. A photograph of the polished aluminium surface before immersion in 1 M HCl solution is shown in Figure 11a. The photograph shows the surface was smooth and without pits. The SEM micrographs of the corroded aluminium in the presence of 1 M HCl solution are shown in Figure 11b. The faceting seen in this figures was a result of pits formed due to the exposure of aluminium to the acid. The influence of the inhibitor addition 300 ppm on the aluminium in 1 M HCl solution is shown in Figure 11c. The morphology in Figure 11c shows a rough surface, characteristic of uniform corrosion of aluminium in acid, as previously reported [52], that corrosion does not occur in presence of inhibitor and hence corrosion was inhibited strongly when the inhibitor was present in the hydrochloric acid, and the surface layer is very rough. In contrast, in the presence of 300 ppm of MOE, there is much less damage on the aluminium surface, which further confirm the inhibition action. Also, there is an adsorbed film adsorbed on aluminium surface (Figure 11c). In accordance, it might be concluded that the adsorption film can efficiently inhibits the corrosion of aluminium.

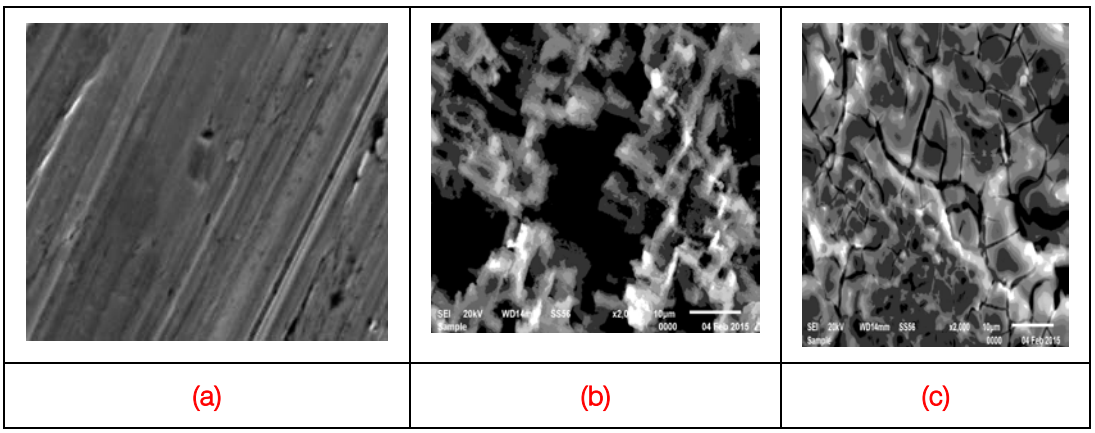

Figure 11: SEM micrographs of aluminium surface (a) before of immersion in 1 M HCl, (b) after 24 h of immersion in 1 M HCl and (c) after 24 h of immersion in 1 M HCl + 300 ppm of MOE at 25°C

i) Mechanism of the corrosion inhibition

The adsorption of organic compounds can be described by two main types of interactions: physical and chemisorptions adsorption. In general, physical adsorption requires the presence of both the electrically charged surface of the metal and charged species in solution. The surface charge of the metal is due to the electric field existing at the metal/solution interface. A chemisorption process, on the other hand, involves charge sharing or charge transfer from the inhibitor molecules to the metal surface to form a coordinate type of a bond. This is possible in case of a positive as well as a negative charge of the surface. The presence of a transition metal, having vacant, low-energy electron orbitals and an inhibitor with molecules having relatively loosely bound electrons or heteroatoms with a lone pair of electrons is necessary for the inhibiting action [53]. Generally, two types of mechanisms of inhibition were proposed. One was the formation of polymeric complexes with aluminium ions (Al^{3+}) depending on the applied conditions[54, 55]. The other was the chemical adsorption of MOE components on aluminium surface

[56, 57]. The inhibition action of MOE does not occur by the simple blocking at the surface of aluminium, especially at high temperature. This might be attributed to the different adsorption capacities of the MOE extract on the aluminium surface at different temperatures. It has been studied that with the increase in temperature, the desorption effect of MOE on aluminium surface increased. Some of the hydrophilic groups with positively charged atoms (O^+) desorbed from the surface of aluminium and did more work to prevent the H^+ from getting nearer to the metal surface. Therefore, MOE preferentially inhibited both cathodic and anodic corrosion processes at high temperature.

IV. Conclusions

From the overall experimental results the following conclusions can be deduced:

1. The MOE shows good performance as corrosion inhibitor in 1 M HCl.
2. The results obtained from weight loss showed that the inhibiting action increases with the MOE concentration and also increase with the increasing in temperature.
3. Double layer capacitances decrease with respect to blank solution when the plant extract is added. This fact confirms the adsorption of plant extract molecules on the aluminium surface.
4. The MOE inhibits the corrosion by getting adsorbed on the metal surface following Temkin adsorption isotherm.
5. The inhibition efficiencies determined by weight loss, potentiodynamic polarization and EIS techniques are in reasonably good agreement.

References Références Referencias

1. Trabanelli G., *Corrosion*, 47 (1991) 410.
2. Singh D. N., Dey A. K., *Corrosion*, 49 (1993) 594.
3. Banerjee G., Malhotra S. N., *Corrosion*, 48 (1992) 10.
4. Arab S. T., Noor E. A., *Corrosion*, 49 (1993) 122.
5. Raspini I. A.,*Corrosion*, 49 (1993) 821.
6. Khadraoui A., Khelifa A., Touafri L., Hamitouche H., Mehdaoui R., *J. Mater. Environ. Sci.* 4 (2013) 663.
7. Elachouri M., Hajji M. S., Salem M., Kertit S., Coudert R., Essassi. E. M., *Corros.Sci.*, 37 (1995) 381.
8. Luo H., Guan Y. C., Han K. N., *Corrosion*, 54 (1998) 619.
9. Migahed M. A., Azzam E. M. S., Al-Sabagh A. M., *Mater. Chem. Phys*, 85 (2004) 273.
10. Villamil R. F. V., Corio P., Rubim J. C., SilivaAgostinho M. L., *J. Electroanal. Chem.*, 472 (1999) 112.
11. Hari Kumar and S. Karthikeyan., *J. Mater. Environ. Sci.* 3 (5) (2012) 925–934.
12. Hadi Z.M. Al-Sawaad, Alaa S.K. Al-Mubarak, Athir M. Haddadl., *J. Mater. Environ. Sci.* 1 (4) (2010) 227-238.
13. Abd El Rehim S. S., Hassan H., Amin M. A., *Mater. Chem. Phys.*, 78 (2003) 337.
14. Guo R., Liu T., Wei X., *Colloids Surf*, *A*, 209 (2002) 37.
15. Branzoi V., Golgovici F., Branzoi F., *Mater.Chem. Phys*, 78 (2002) 122.
16. Parikh K. S., Joshi K. J., *Trans. SAEST*, 39 (2004) 29.
17. Al-Mhyawi S. R, Orient Journal of Chemistry, 30 (2014) 3760.
18. A. I. Ali and N. Foaud., J. Mater. Environ. Sci., 3 (5) (2012) 917-924.
19. Nwosu O. F., Osarolube E., Nnanna L. A., Akoma C. S., Chigbu T. American Journal of Materials Science 4(4) (2014) 178-183.
20. A. O. James and O. Akaranta. African Journal of Pure and Applied Chemistry., 3 (12) (2009) 262-268.
21. Nicole Kresge, Robert D. Simoni, and Robert L. Hill. /5% "Hemorrhagic Sweet Clover Disease, Dicumarol, and Warfarin: the Work of Karl Paul Link". Retrieved 2009-08-11.
22. "BSBI List 2007" (xls). Botanical Society of Britain and Ireland. Archived from the original on 2015-02-25. Retrieved 2014-10-17.
23. Abd-El-Nabey B. A., Abdel-Gaber A. M., El. Said Ali M., Khamis E., El-Housseiny S., *J. Electrochem. Sci.*, 8(2013) 5851.
24. A.I. Onuchukwu, The kinetic and mechanism of hydrogen evolution on corroding aluminium in alkaline medium, Mater. Chem. Phys. 25, (1998) 227-235.
25. El Sheikh M. O. A., El Hassan G. M., El Tayeb A. H., Abdallah A. A., Antoun M. D., 1982. Studies on Sudanese medicinal plants III: indigenous Hyoscyamusmuticus as possible commercial source for hyoscyamine. PlantaMedica 45: 116–119.
26. Eeva M., Salo J. P., Oksman-Caldentey K. M., *J Pharm Biomed Anal*. 1998; 16(5):717. "Determination of the main tropane alkaloids from transformed Hyoscyamusmuticus plants by capillary zone electrophoresis".
27. Mu G. N., Zhao T. P., Liu M., Gu T., *Corrosion*, 52 (1996) 853.
28. Parr R. G., Donnelly R. A., Levy M. Palke W. E., *J. Chem. Phys*., 68 (1978) 3801.
29. Bosch R. W., Hubrecht J., Bogaerts W. F., Syrett B. C., *Corrosion*, 57(2001) 60.
30. Zhang D. Q., Cai Q. R., He X. M., Gao L. X., Kim G. S., *Mater. Chem. Phys*. 114 (2009) 612.
31. Lee H. P., Nobe K., *J. Electrochem. Soc*. 133 (1986) 2035.
32. Tao Z. H., Zhang S. T., Li W. H., Hou B. R.,*Corros. Sci*.51 (2009) 2588.
33. Ferreira E. S., Giacomelli C., Giacomelli, F. C., Spinelli A., *Mater. Chem. Phys*. 83 (2004) 129.

34. Paskossy T., *J. Electroanal. Chem*, 364 (1994) 111.
35. Growcock F. B., Jasinski J. H., *J. Electrochem. Soc*., 136 (1989) 2310.
36. Abd El-Rehim S. S., Khaled K. F., Abd El-Shafi N. S., *Electrochim. Acta*, 51 (2006) 3269.
37. Metikos M., Hukovic R., Bobic Z. Gwabac S., *J. Appl. Elactrochem*., 24 (1994) 772.
38. Caprani A., Epelboin I., Morel Ph., TakenoutiH., *proceedings of the 4th European sym. on Corros. Inhibitors*, (1975) 571.
39. Bessone J., Mayer C., TuttnerK., Lorenz W. J., *Electrochim. Acta*, 28 (1983) 171.
40. Epelboin I., Keddam M., Takenouti H., *J. Appl. Electrochem*., 2 (1972) 71.
41. Benedeti A. V., Sumodjo P. T. A., Nobe K., Cabot P. L., Proud W. G., *ElectrochimicaActa*, 40 (1995) 2657.
42. Ma H., Chen S., Niu L., Zhao S., Li S., Li D., *J. Appl. Electrochem.* 32 (2002) 65.
43. Li X. H., Deng S. D., Fu H., *J. Appl. Electrochem*., 40 (2010) 1641.
44. Lagrenee M., Mernari B., Bouanis M., Traisnel M., Bentiss F., *Corros. Sci*., 44 (2002) 573.
45. Kus E., Mansfeld F., *Corros. Sci*., 48 (2006) 965.
46. Caigman G. A., Metcalf S. K., Holt E. M., *J. Chem. Cryst*, 30 (2000) 415.
47. Abdel–Rehim S. S., Khaled K. F., Abd–Elshafi N. S., *Electrochim. Acta*, 51 (2006) 3269.
48. Bockris J. O., Swinkels D. A. J., *J. Electrochem. Soc*., 111 (1964) 736.
49. Lorenz, W. J., Mansfeld F., Corros. *Sci.,* 21 (1981) 647.
50. Yurt A, Bereket G, Kivrak A, Balaban A &Erk B, *J Appl Electrochem*, 35 (2005) 1025.
51. 26. Bentiss F, Traisnel M & Lagrenee M, *Corros Sci.,* 42 (2000) 127.
52. Saleh M. M., Atia A. A., *J. Appl. Electrochem*., 36 (2006) 899.
53. Narvez L., Cano E., Bastidas D. M., *J. Appl. Electrochem*., 35 (2005) 499.
54. Li X. H., Deng S. D., Fu H., *Corros. Sci*., 51 (2009) 1344.
55. Putilova I. K., Balezin S. A., Barasanik Y. P., *Metallic Corrosion Inhibitors, Oxford: Pergamon Press,* (1960) 30.
56. Saliyan V. R., Adhikari A. V., *Bull. Mater. Sci*., 31 (2007) 699.
57. Li Y., Zhao P., Liang Q., Hou B., *Appl. Surf. Sci*., 252 (2005) 1245.
58. Mehaute A. H., Grepy G., *Solid State Ionics*, 9–10 (1989) 17.
59. Brusic V., Frisch M. A., Eldridge B. N., Novak F. P., Kauman F. B., Rush B. M., Frankel G. S., *J. Electrochem. Soc*. 138 (1991) 2253.
60. Antonijevic M. M., Petrovic M. B., *Int. J. Electrochem. Sci.* 3 (2008) 1.
61. Musiani M. M., Mengoli G., *J. Electroanal. Chem*. 217 (1987) 187.
62. Lewis G., *Corrosion* 34 (1978) 424.